Overlapping β decay and resonance neutron spectroscopy of levels in ^{87}Kr

S. Raman, B. Fogelberg,* J. A. Harvey, R. L. Macklin, and P. H. Stelson
Oak Ridge National Laboratory, Oak Ridge, Tennessee 37830

A. Schröder and K.-L. Kratz
Institut für Kernchemie, Universität Mainz, D-65 Mainz, Federal Republic of Germany
(Received 4 March 1983)

Energy levels in ^{87}Kr have been studied, with special emphasis on the unbound region, using two different methods. The first method comprises neutron capture and transmission measurements on an enriched gas target of ^{86}Kr using neutron time-of-flight techniques. In this way, neutron widths were determined for 39 resonances below 400 keV and capture areas for 14 resonances below 90 keV. The second method is a decay study of 56-s ^{87}Br in which a level scheme for ^{87}Kr has been established that shows 126 levels in the bound and 12 levels in the unbound region. A detailed comparison amongst the neutron resonance, the γ-ray decay, and available delayed neutron results has been made. Almost a one-to-one correspondence exists between the currently observed p-wave resonances below 250 keV and levels in ^{87}Kr studied through delayed neutron emission. The overall β-strength distribution derived from the present data shows broad resonancelike structures. However, no marked selectivity is observed in the β decay to individual levels in the unbound region of ^{87}Kr. The neutron capture cross section of ^{86}Kr is found to be about 5 mb for 30-keV neutrons with a Maxwellian energy distribution. The future of delayed neutron spectroscopy as a new tool for obtaining level-density information is discussed.

[NUCLEAR REACTIONS ^{86}Kr(n), E_n=1–400 keV, measured total $\sigma(E)$; ^{86}Kr(n,γ), E_n=1–90 keV, measured $\sigma_{n\gamma}$; ^{87}Kr deduced resonances, resonance parameters, neutron strength functions, Maxwellian average cross section; enriched target.
RADIOACTIVITY ^{87}Br [from ^{235}U(n,f)], measured E_γ, i_γ, $\gamma\gamma$-coinc; deduced ^{87}Kr levels; deduced ^{87}Br ground state J, π; Ge(Li) detector, mass separated source.]

I. INTRODUCTION

The properties of the ^{86}Kr + n system (see Fig. 1) are of considerable interest since the nucleus ^{87}Kr is the daughter of the delayed neutron precursor ^{87}Br. The latter nucleus is, from systematics, believed to have a ground-state spin and parity of $3/2^-$. Consequently, the unbound levels in ^{87}Kr with $J^\pi = 1/2^-$ and $3/2^-$, which are populated in the allowed β^- decay of ^{87}Br, can also be seen as p-wave resonances in high-resolution measurements of the neutron cross sections of ^{86}Kr. The β decay also populates $5/2^-$ levels, which are however too narrow to be observed as (f-wave) neutron resonances even with the best of the present-day facilities. These levels may instead, at least for moderate excitation over the binding energy, be observed as γ-decaying states in decay scheme studies.

Much of the existing information on nuclear level densities comes from resonance neutron spectroscopy. This technique is generally restricted to stable or nearly stable targets. For the majority of nuclides which lie further away from stability, it is necessary to resort to indirect information from β-decay studies (delayed particle emission, γ-ray spectra, etc.) in order to extract information on level densities. The validity and reliability of the latter approach can be tested in the case of ^{87}Kr because many of the unbound levels in this nucleus are accessible to both β decay and resonance neutron spectroscopy. Such an opportunity occurs very rarely throughout the periodic table.

The indirect level-density information gleaned from β-decay studies is hampered by two main drawbacks. The first is that it is not known with sufficient certainty whether the reduced β probabilities obey, as do the neutron widths, a Porter-Thomas distribution (a χ^2 distribution with one degree of freedom). The second concerns the limited resolution attained in delayed neutron spectroscopy. For instance, the most detailed neutron spectrum[1] from the decay of ^{87}Br obtained so far has a resolu-

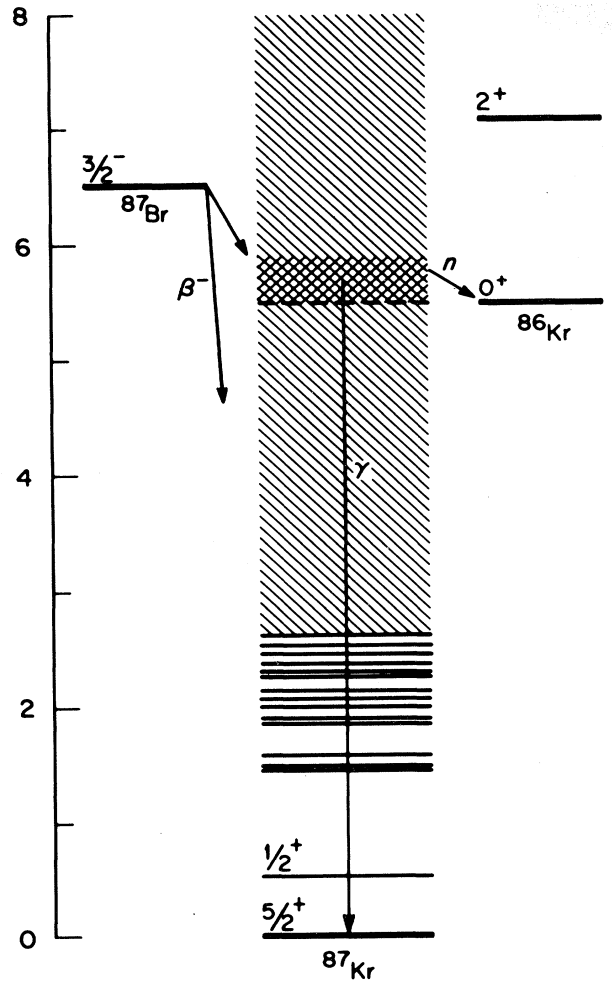

FIG. 1. A schematic drawing showing the β decay of ^{87}Br, the bound and unbound levels in ^{87}Kr, and the ^{86}Kr + n system, all of which have been studied in the present experiment. The energy scale on the left is in MeV.

tion of about 15 keV for the range $0 < E_n < 500$ keV. In a peak-fitting analysis,[1] about 85% of the neutron intensity was accounted for by the peaks observed in the spectrum which were interpreted as individual transitions. This interpretation has caused some debate about the significance of the structure of the peaks in delayed neutron spectra. Statistical calculations performed by Gjøtterud *et al.*[2] and Hardy *et al.*[3] suggest that because of the expected high density of levels populated in β decay, the peaks observed in delayed particle spectra of medium mass nuclei are not in general representative of individual transitions but result from the summation within the detector resolution of many randomly spaced lines. Other workers,[1,4,5] however, claim (1) that, at least for selected neutron precursors like ^{87}Br, these complications are minimized and (2) that in certain cases delayed neutron spectroscopy, even with the moderate resolution available today, would offer a new method for studying individual levels at high excitation energy. (In the case of ^{87}Br, Hardy *et al.*[3] do mute their strong criticism of inferences drawn from studies of delayed neutron spectra.)

The main goal of the present study has been to tackle the above issues by providing data for an accurate determination of the level density in ^{87}Kr for the first few hundred keV above the binding energy and by comparing high-resolution neutron cross-section results with the delayed neutron spectrum[1] and with the unbound part of the γ-ray decay scheme of ^{87}Br. A detailed decay scheme investigation including coincidence studies was necessary in order to significantly improve the existing scheme. The high-lying part of the decay scheme, when compared to the level density from the cross-section study, would permit a more definitive test than the one performed by Nuh *et al.*[1] of possible nuclear-structure-dependent selectivity of β decay to levels in this region of excitation.

Another goal has been to determine the neutron capture cross section of ^{86}Kr in the energy region of interest from the astrophysical point of view. The properties of ^{86}Kr, which is the heaviest of the stable Kr nuclei and which has no stable neighbor isotope, are of interest[6,7] for calculations of nucleosynthesis. The stellar average cross section, only ~5 mb, is exceptionally small. Of all the isotopes involved in *s*-process nucleosynthesis, only doubly magic ^{208}Pb has a significantly smaller cross section than does ^{86}Kr. Previous studies of the neutron cross sections of Kr isotopes made by Käppeler and Leugers[8] and by Maguire *et al.*[9] did not include resonances in ^{86}Kr. The data of Ref. 8 could be employed however to identify two weak resonances observed in the present measurement as being caused by ^{84}Kr, which comprised about 0.5% of the ^{86}Kr sample.

II. EXPERIMENT AND DATA ANALYSIS

A. Neutron capture and transmission

The measurements were made at the Oak Ridge electron linear accelerator (ORELA). For these measurements, the 140–170-MeV electron beam was pulsed at 800 pulses/s with a peak current of about 10 A at a pulse width of 5–8 ns. The electron beam struck a water-cooled Ta target with dimensions of about 3.2×3.2×5 cm which released

about 1×10^{10} photoneutrons per pulse.

The neutron capture measurements were made at the 40-m flight path using the capture cross-section facility described earlier.[10] The energy resolution, $\Delta E/E$, was $\approx 1/700$ for the region of interest here. This good resolution enabled capture in individual resonances to be distinguished from background. The 99.5% enriched ^{86}Kr gas was contained at a pressure of about 2 MPa in a thin ($\sim$0.12-mm wall), cylindrical, stainless steel sample cell made to fit into the automatic sample-changing mechanism. An area of 2.9×5.7 cm^2 containing 3.63 g of ^{86}Kr was exposed to the neutron beam. The greater part of the observed signal resulted from resonances in iron, nickel, and chromium present in the sample cell. The cell containing the ^{86}Kr was emptied to make a "background" subtraction, but the sample-cell effect was nevertheless so severe that statistically significant subtracted data were obtained for resonances only below 90 keV. The lowest energy resonance was found at 5.61 keV (see Fig. 2 and Table I). A special run emphasizing the low-energy region showed that no resonances were present below this one.

The neutron capture data were analyzed with a computer program[11] which allows for corrections for experimental resolution, Doppler broadening, resonance self-protection, and multiple scattering. The slight asymmetry [see Fig. 2(a)] in the resolution function was mostly caused by the water moderator and was modeled in peak fitting by convoluting part of the Gaussian resolution function with an exponential. For most resonances, the values of E_0 and $g\Gamma_n$ were well known from the transmission measurements and were kept fixed in the analysis. Two resonances were, however, seen only in the neutron capture experiments (see Table I). The capture areas, $A_\gamma = 2\pi^2 \lambda\!\!\!^{-2} g\Gamma_n\Gamma_\gamma/\Gamma$ ($\lambda\!\!\!^{-}$ and

TABLE I. Parameters for resonances in ^{86}Kr below 90 keV.

E_n[a] (keV)	ℓ[b]	J^π[b]	$g\Gamma_n$[c] (eV)	$g\Gamma_n^{ld}$[d] (eV)	$g\Gamma_n\Gamma_\gamma$[e]/Γ (eV)	$g\Gamma_\gamma$[f] (eV)	Γ_γ[g] (eV)
5.609					0.024[h] *2*		
11.629					0.026[h] *3*		
19.229	1	$1/2^-,3/2^-$	14.7 *4*	3.37 *10*	0.17 *2*	0.17 *2*	
25.829			1.5 *3*		0.23 *2*	0.27 *3*	
27.845	1	$1/2^-,3/2^-$	15.7 *5*	2.10 *7*	0.22 *4*	0.22 *4*	
36.930	0	$1/2^+$	53 *2*		0.30 *8*	0.30 *8*	0.30 *8*
43.913	1	$1/2^-$	125 *4*	8.64 *28*	0.39 *10*	0.39 *10*	0.39 *10*
48.659			2.1 *8*		0.32 *6*	0.38 *9*	
49.640	0	$1/2^+$	42 *3*		0.20 *6*	0.20 *6*	0.20 *6*
54.372	1	$3/2^-$	402 *10*	20.5 *5*	1.1 *3*	1.1 *3*	0.55 *15*
68.613	1	$1/2^-,3/2^-$	25 *3*	0.92 *11*	0.14 *7*	0.14 *7*	
78.862	1	$1/2^-$	95 *5*	2.88 *16*	0.33 *12*	0.33 *12*	0.33 *12*
79.392			9.8 *9*		0.35 *9*	0.35 *9*	
88.270			4 *2*		0.46 *16*	0.52 *21*	

[a]Resonance energies, based on absolute neutron time of flight, are accurate to $\approx$ 0.08%.

[b]From a detailed analysis of the magnitude and shape of the transmission dip.

[c]From the area of the transmission dip. In our notation, 14.7 *4* $\equiv$ 14.7 $\pm$ 0.4, etc.

[d]Reduced neutron width for p-wave neutrons based on a nuclear radius of 5.98 fm.

[e]From capture cross section measurements.

[f]Deduced from $g\Gamma_n$ and $g\Gamma_n\Gamma_\gamma/\Gamma$ values.

[g]Total radiation width calculated for those resonances with definite g values. $g = 1$ if $J = 1/2$ and $g = 2$ if $J = 3/2$ for the present case.

[h]Seen only in capture measurements. Since Γ_γ is typically $\approx$0.3 eV, these values represent $g\Gamma_n$ values.

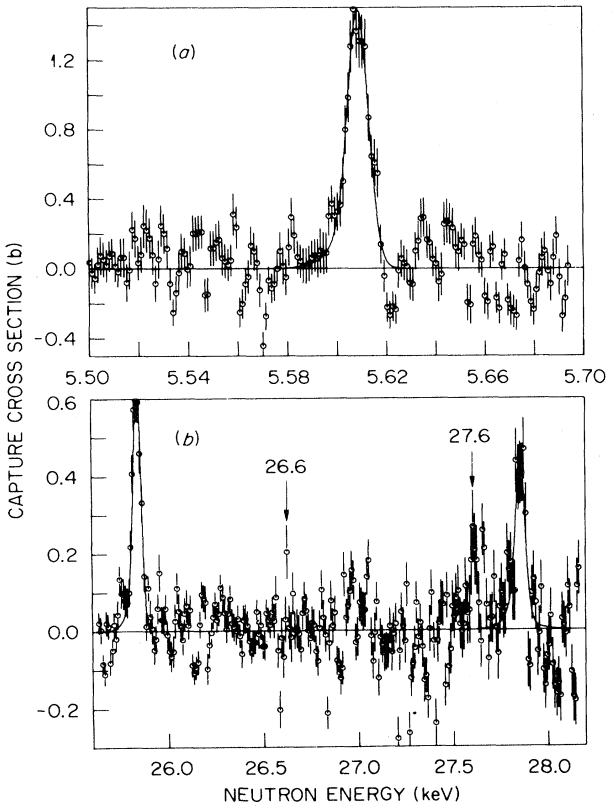

FIG. 2. Some examples of the data from the neutron capture measurements. The resonance shown in (a) was seen in only the capture study. The considerable scatter in the data points at 26.6 and 27.6 keV is due to the subtraction of the capture contribution from the stainless steel sample cell, which showed prominent resonances at these energies. The capture areas are listed in Table I.

g are defined below), obtained in the analysis were further corrected for the effect of neutrons having been resonantly scattered into the γ-ray detectors. This effect has been discussed in previous publications (see, e.g., Ref. 12). The corrections were made using the known $g\Gamma_n$ values and were small in most cases. The exact magnitude of this effect is difficult to estimate. Hence, an additional uncertainty amounting to 50% of the correction has been assigned to the capture areas.

The neutron transmission measurements for obtaining the total cross-section data were made at a flight path of 80.5 m. Here, the ^{86}Kr gas was kept at a pressure of about 2.7 MPa in a cylindrical sample cell 30.2 cm in length. The cell was equipped with thin end windows of stainless steel. The inner diameter of the cell was 1.08 cm. This diameter gave sufficient room for the neutron beam, which was collimated to 0.953 cm diam. Because only the thin end windows of the cell were exposed to the beam, a much smaller cell effect was encountered than occurred in the capture study, and this effect could be precisely balanced out by frequently exchanging the cell holding the ^{86}Kr gas for a blank one. The thickness of ^{86}Kr traversed by the beam was determined as 0.0210 atoms/b from the peak cross sections of broad resonances and from an independent weight determination.

The data obtained were analyzed up to 400 keV neutron energy. The energy resolution, $\Delta E/E$, was $\approx 1/1000$. Figure 3 shows the deduced experimental total cross section covering this region. A computer code, SAMMY,[13] based on multilevel formalism and incorporating many of the features from an earlier code, MULTI,[14] was used to extract values of E_0 and $g\Gamma_n$ for the resonances. An important aspect of SAMMY is that it allows the user to simulate the effect of resonances or of bound states

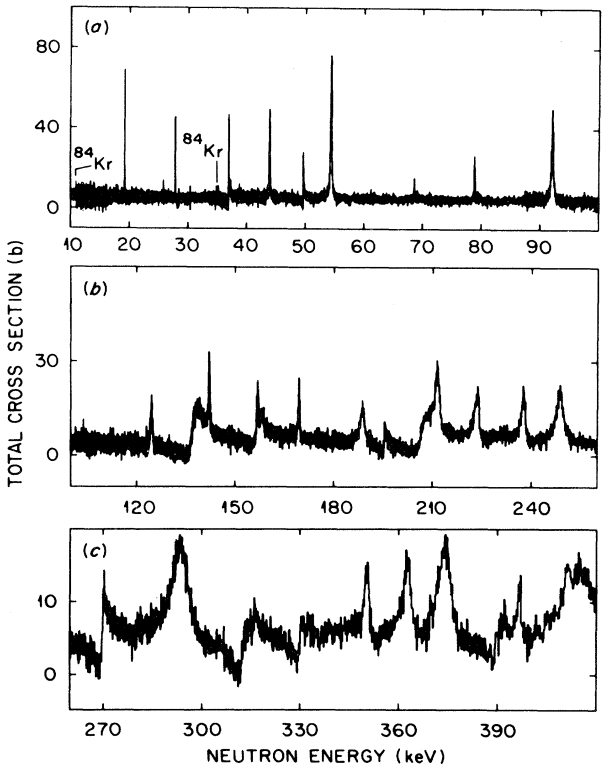

FIG. 3. The total cross-section curve for ^{86}Kr as deduced from the transmission measurements. The top panel has a higher energy dispersion than do the other two. The resonance parameters are given in Tables I and II.

outside the region studied by a smoothed average external R function for each J^π value. The two parameters describing the external R function are fitted by the program. The application of average external R functions in the analysis of high-resolution neutron cross-section data has recently been discussed by Johnson and Winters.[15] This feature reproduces interference effects very well and is an alternate method to the use of dummy resonances outside the region being analyzed. The code makes corrections for instrumental and Doppler broadening. Examples of multilevel fits are given in Fig. 4. The bottom part of this figure shows one of the two cases where a resonance was found to be a doublet, that is, comprising two components with different spins and/or parities. The resonance parameters extracted from the transmission data are given in Tables I and II.

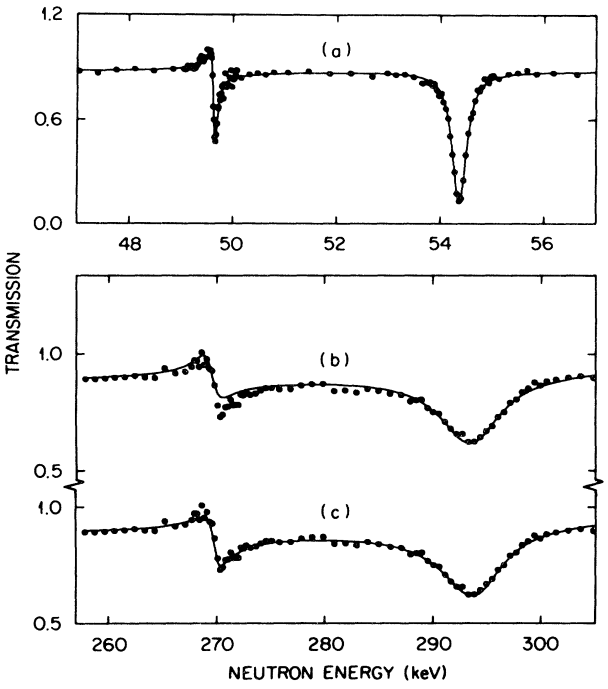

FIG. 4. Some examples of multilevel fits (solid lines) to the transmission data. In regions away from resonances, the points shown are averages of several data points. Curve (a) illustrates the strong interference between potential and resonance scattering for an s-wave resonance near 49 keV and the absence of such interference for a p-wave resonance near 54 keV. The two lower curves show one of the two cases where the multilevel fitting procedure showed a resonance to be a doublet. The shape of an s-wave resonance only, curve (b), was insufficient to fill the transmission dip near 270 keV. A $p_{1/2}$ contribution was also needed to reproduce the experimental transmission data as shown by curve (c). The relatively poor fit below the resonance is not considered serious.

B. Decay scheme of ^{87}Kr

The levels in ^{87}Kr populated in the β decay of ^{87}Br [$T_{1/2}$ = 55.69 ± 0.13 s] were studied in a straightforward way by measurements of γ-ray singles and $\gamma\gamma$–coincidence spectra. The ^{87}Br activity

TABLE II. Neutron widths for resonances in ^{86}Kr above 90 keV.

E_n[a] (keV)	ℓ	J^π[b]	$g\Gamma_n$[c] (keV)	$g\Gamma_n$[1d] (eV)
92.11	1	$3/2^-$	0.64 *3*	15.6 *8*
124.53	1	$1/2^-$	0.39 *3*	6.4 *5*
137.42	0	$1/2^+$	2.93 *8*	
142.07	1	$3/2^-$	0.51 *3*	7.0 *5*
156.85	1	$3/2^-$	0.97 *4*	11.7 *5*
157.62	0	$1/2^+$	0.81 *4*	
169.37	1	$3/2^-$	0.58 *3*	6.4 *4*
188.55	1	$1/2^-$	1.32 *6*	12.6 *6*
195.37	0	$1/2^+$	0.28 *3*	
206.87	0	$1/2^+$	5.30 *25*	
211.45	1	$3/2^-$	2.67 *22*	22.0 *19*
223.52	1	$3/2^-$	2.30 *20*	17.8 *16*
237.59	1	$3/2^-$	2.41 *25*	17.3 *18*
248.59	1	$3/2^-$	5.07 *23*	34.4 *16*
270.07[e]	1	$1/2^-$	0.93 *10*	5.7 *7*
270.28[e]	0	$1/2^+$	1.98 *16*	
293.32	1	$3/2^-$	12.60 *40*	70.5 *23*
312.82	0	$1/2^+$	3.70 *19*	
316.36	1	$(3/2)^-$	0.24 *3*	1.2 *2*
329.83	0	$1/2^+$	1.43 *15*	
350.45	1	$3/2^-$	3.91 *20*	17.8 *9*
362.87	1	$3/2^-$	7.12 *30*	31.1 *14*
373.03	1	$3/2^-$	11.30 *50*	48.1 *22*
374.66	1	$1/2^-$	2.00 *60*	8.4 *26*
389.11	0	$1/2^+$	0.37 *4*	
392.29	1	$1/2^-$	0.76 *8*	3.1 *4*
396.90	1	$3/2^-$	2.34 *20*	9.3 *8*

[a]Resonance energies, based on absolute neutron time of flight, are accurate to ≈ 0.08%.
[b]From a detailed analysis of the magnitude and shape of the transmission dip.
[c]From the area of the transmission dip. In our notation, 0.64 *3* ≡ 0.64 ± 0.03, etc.
[d]Reduced neutron width for p-wave neutrons based on a nuclear radius of 5.98 fm.
[e]See Fig. 4 and related discussion.

was continually produced by means of thermal fission of ^{235}U in the ion source of the OSIRIS mass-separator facility[16] located at the R2-0 reactor in Studsvik. The mass-separated beam at $A = 87$ contained almost exclusively ^{87}Br and ^{87}Kr because the ion source used had a very low efficiency for the shorter-lived elements in this isobaric chain. In the singles γ-ray measurements, the activity was collected on a tape of Al-coated Mylar for periods of 110 s, after which the tape was moved 35 cm to a shielded position and viewed by a Ge(Li) detector. A source-to-detector distance of 10 cm was used; this distance ensured that true coincidence summing was kept to a negligible level. The β particles emitted by the ^{87}Br activity were stopped in a 4-cm thick disc of perspex inserted between the source and the detector. Because the experiment also aimed at identifying very weak lines following the decay of ^{87}Br, the background and possible contaminations were carefully investigated. Furthermore, the decay period of each γ line was checked by measuring two consecutive spectra from each collected source and routing these spectra to different parts of the computer memory. The fact that the collected sources of ^{87}Br also emitted several thousand delayed neutrons per second necessitated a special search for possible background (n,γ) lines following the same half-life as the ^{87}Br lines. No such lines were found, however. Examples of γ-ray spectra are shown in Fig. 5.

The $\gamma\gamma$–coincidence study was made using a geometry in which two Ge(Li) detectors viewed the position where the activity was collected on the tape. The tape was moved slowly for removal of the daughter activity. The counting rate was never allowed to exceed 4000 counts/s in each detector; this rate ensured a reasonable ratio between true and random coincidences. The coincidence resolving time, 2τ, was 10 ns. The measurement lasted 92 h.

The γ-ray spectrum of ^{87}Br is relatively complex (see Fig. 5). Table III gives the results of the γ-ray measurements. Coincidence gates were selected and analyzed for each of the $\approx$220 γ rays judged to be above the detection limit in the coincidence measurements. The results are presented in Table IV. The energies and intensities of several lines which were unresolved in the singles measurements were deduced from the coincidence data. A number of reasonably strong γ lines were found to have no coincidence relationships with other transitions. These are all likely to be transitions to the ground state because no isomerism is expected in ^{87}Kr.

The complete decay scheme is presented in Table V. The Q_β value of 6.83 $\pm$ 0.12 MeV is from Ref. 17. The γ-ray intensities in Table III have been normalized to the absolute intensity of 22.0 $\pm$ 1.5% found[18] for the 1419.7-keV γ ray. This value is based on β-ray and γ-ray measurements with detectors of known absolute efficiencies and may be compared with values of 31% and 12% reported in Refs. 1 and 19, respectively. The β^- intensities were deduced from the measured photon intensities, the requirement that the intensity feeding the ground state is 100, and the intensity balance at each level. The deduced β^- intensities (nonzero within 3 standard deviations) and log ft values are given in Table VI, but it must be understood that because the decay scheme is complex, many β branches indicated there may not actually exist, especially those very weak branches deduced for low-lying levels from intensity balance requirements.

All γ rays with energies below about 5 MeV which have been placed in the decay scheme have their position in the scheme supported by the coincidence measurements. The present decay scheme is therefore better established than previous ones.[1,19,20] As mentioned above, strong γ rays not in coincidence with other γ rays have been taken to represent transitions to the ground state. The γ rays with energies greater than 5 MeV are all assumed to be transitions to the ground state. This assumption is supported by the coincidence data for all but ten of the transitions. However, these latter ten are so weak that possible coincidences with the radiations deexciting the first few excited states could have escaped detection. On the other hand, if these γ rays are not taken to be ground-state transitions, the corresponding level energies would be so high above the neutron separation energy that detectable γ decay would be highly improbable.

Very few levels of ^{87}Kr have known spin and parity assignments. In transfer reactions,[21,22] the ground state and first excited level have been shown to be $J^\pi = 5/2^+$ and $1/2^+$, respectively, and l values have been obtained in these works for a number of additional levels below 3.3 MeV. The 1476-keV level is suggested to have $J^\pi = 3/2^+$ from a thermal neutron capture study.[23] This study also gives the neutron binding energy of ^{87}Kr as $S_n = 5515.4 \pm 0.8$ keV.

The spin and parity of the β-decaying ground state of ^{87}Br is most probably $3/2^-$, as discussed in Sec. III C below. One can thus expect that only those levels in ^{87}Kr with spins of 1/2, 3/2, and

5/2, respectively, will receive substantial population in the β decay of ^{87}Br. The level scheme information does not provide a means of discerning the different spin values. For the majority of the levels, even the parity remains undetermined. Reliable parity assignments can be made only for levels populated by β transitions that undoubtedly are allowed, with values of log ft below[24] 5.9. Only a few levels at relatively high excitation energy are populated by such strong transitions.

A number of levels in the level scheme are present in the region above the neutron binding energy. These are all taken to be $J^\pi = 5/2^-$ on grounds discussed below in Sec. III C.

III. DISCUSSION

A. Spin and parity determinations for resonances

Because the ground state of ^{86}Kr has $J^\pi = 0^+$, interactions with s-wave neutrons form $1/2^+$ reso-

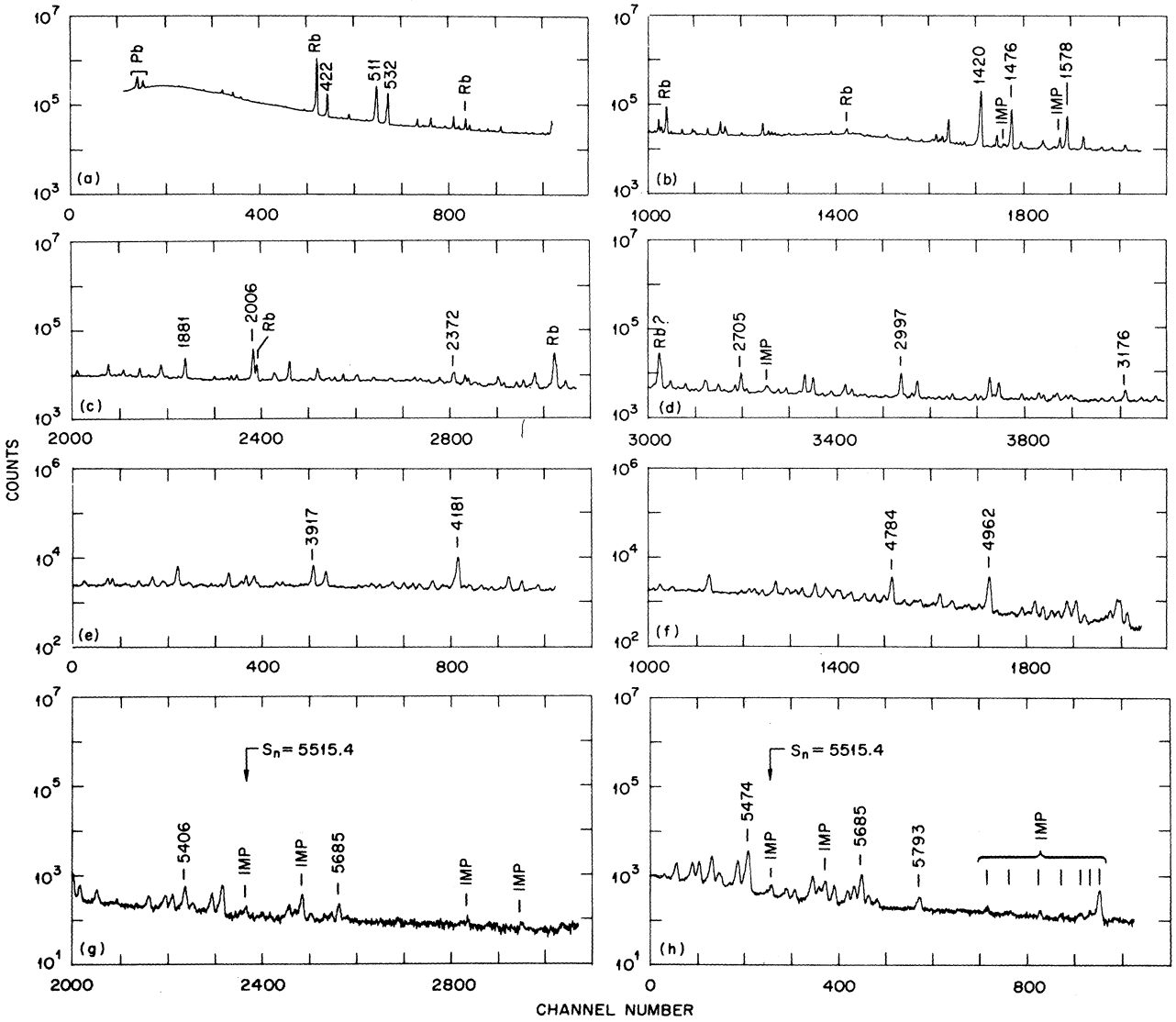

FIG. 5. An example of a γ-ray spectrum from the $A = 87$ isobars recorded at the OSIRIS facility. For practical reasons, only a fraction of the lines following the decay of ^{87}Br have been labelled by their γ-ray energies. All visible transitions in ^{87}Rb resulting from daughter activity have, however, been indicated, as well as background and impurity lines. The latter have been labelled "IMP" regardless of their origin. Parts (a) through (g) are consecutive; part (h) is a separate run emphasizing the high-energy region. Gamma rays higher than 5515.4 keV represent transitions from unbound levels.

TABLE III. Energies and intensities of γ rays following the decay of ^{87}Br.

Energy[a] (keV)		Intensity[b]		Energy[a] (keV)		Intensity[b]		Energy[a] (keV)		Intensity[b]		Energy[a] (keV)		Intensity[b]	
93.54[c]	7	0.130	9	1041.77[c]	10	0.076	10	1781.17[c]	40	0.13	4	2570.81[c]	30	0.12	2
121.42[c]	7	0.036	4	1043.3	6	0.12	4	1796.2[c]	7	0.14	9	2575.37	9	0.58	5
175.59[c]	10	0.052	9	1044.3	6	0.06	2	1798.31	7	0.60	4	2590.03[c]	15	0.13	1
190.29[c]	7	0.078	10	1060.69[c]	15	0.089	10	1831.49[c]	30	0.20	2	2596.32[c]	30	0.099	10
230.33	9	0.54	4	1064.75[c]	15	0.075	10	1836.78	7	1.4	1	2603.20	8	0.41	3
263.96	7	0.20	2	1078.88	9	0.10	1	1840.10	15	0.38	4	2607.13[c]	30	0.081	10
346.06[c]	7	0.080	6	1095.16	15	0.093	10	1847.34[c]	30	0.12	2	2622.77[c]	15	0.053	6
380.14[c]	7	0.15	1	1099.88	10	0.099	10	1868.72	30	0.13	2	2638.7	4	0.43	7
389.14[c]	20	0.031	6	1113.05[c]	20	0.044	9	1881.20	20	1.9	2	2639.0	6	0.12	4
421.74	10	3.2	3	1120.19[c]	15	0.072	9	1882.2	4	0.60	10	2641.67	8	0.59	5
447.61[c]	15	0.10	2	1126.78	15	0.085	10	1899.89[c]	40	0.05	1	2662.79	15	0.34	5
454.4[c]	5	0.031	10	1139.72[c]	40	0.044	9	1906.84[c]	30	0.076	10	2688.79[c]	15	0.033	20
461.52	7	0.43	3	1146.2	6	0.16	4	1934.67	8	0.22	2	2693.94	10	0.41	3
493.39[c]	7	0.100	9	1146.3	6	0.15	4	1947.93[c]	30	0.084	20	2704.88	7	1.7	1
529.60	15	1.3	2	1186.27[c]	10	0.13	2	1953.57[c]	40	0.064	10	2709.16[c]	30	0.13	2
532.03	7	5.4	4	1198.11[c]	30	0.064	10	1958.23	15	0.16	2	2715.19	10	0.19	2
555.72	7	0.047	4	1212.60	9	0.19	2	1965.58	9	0.22	5	2744.7[c]	6	0.013	3
583.6[c]	5	0.09	3	1220.66[c]	40	0.038	10	2005.52	7	5.3	4	2754.3	4	0.24	3
600.44[c]	15	0.086	10	1225.58[c]	15	0.091	20	2022.62[c]	30	0.11	2	2811.3[c]	6	0.16	4
610.46	7	0.60	6	1255.1[c]	5	0.11	3	2035.42[c]	15	0.077	8	2820.97	7	1.8	1
611.5	8	0.24	6	1276.41[c]	40	0.045	10	2066.32[c]	30	0.15	3	2828.79	20	0.20	2
614.2[c]	9	0.05	3	1285.66	9	0.22	4	2071.66	7	2.3	2	2836.36	7	1.4	1
617.49	30	0.12	4	1291.7	2	0.11	1	2080.91[c]	40	0.086	20	2853.35[c]	15	0.089	8
636.39	8	0.16	1	1298.6[c]	5	0.058	20	2092.84[c]	15	0.058	7	2862.91[c]	40	0.065	10
651.96	7	1.10	8	1311.21	10	0.16	2	2107.90[c]	20	0.13	2	2869.20	15	0.24	2
681.22	8	0.38	3	1330.43	15	0.14	2	2110.23[c]	15	0.099	10	2889.8	4	0.10	2
685.9[c]	7	0.038	20	1338.03	7	0.74	5	2119.90[c]	30	0.19	6	2901.0[c]	5	0.086	20
692.50[c]	40	0.031	2	1344.60	15	0.21	2	2122.62	9	1.20	9	2907.46	15	0.40	4
698.59	9	0.14	1	1349.19	7	0.45	3	2125.85	20	0.19	3	2914.6[c]	7	0.088	20
714.09	7	0.19	1	1355.1	6	0.10	3	2138.71[c]	30	0.12	2	2922.57[c]	40	0.10	2
719.46[c]	10	0.060	7	1356.0	6	0.07	2	2143.40	15	0.25	3	2925.62[c]	30	0.033	7
724.57	15	0.082	10	1360.59	20	3.4	2	2169.30	7	0.55	4	2931.64[c]	15	0.14	4
737.96	7	0.47	3	1366.44[c]	40	0.062	20	2175.42[c]	30	0.088	20	2942.97	30	0.077	10
798.64[c]	30	0.038	9	1376.08	15	0.10	1	2192.46	10	0.31	4	2967.05[c]	10	0.063	30
823.97	30	0.12	2	1389.77	7	0.11	3	2226.11	30	0.15	3	2970.8[c]	8	0.093	30
831.26	7	1.30	9	1415.43	15	1.5	2	2254.23[c]	15	0.19	2	2997.21	7	2.3	2
834.85[c]	40	0.17	7	1419.71	7	22.0	15	2258.44	10	0.15	1	3003.91	30	0.12	1
853.6	6	0.10	4	1436.18[c]	40	0.021	5	2299.93	8	0.31	2	3017.39	15	0.27	2
853.8	6	0.05	2	1443.21	15	0.14	2	2318.62[c]	30	0.051	10	3026.77	7	1.30	9
860.00[c]	15	0.020	3	1449.24	7	1.10	8	2339.90[c]	15	0.12	1	3039.92[c]	40	0.047	10
874.30	7	0.39	3	1464.95[c]	15	0.16	3	2345.3	4	0.37	6	3048.04	20	0.10	1
878.3[c]	5	0.028	9	1471.68[c]	15	0.44	5	2345.4	6	0.12	4	3066.85	15	0.13	1
889.9[c]	7	0.063	30	1476.06	7	7.9	6	2369.39	10	0.56	8	3080.72	15	0.17	2
893.42	9	0.40	3	1488.39[c]	10	0.015	9	2372.38	7	1.00	8	3090.8	6	0.09	3
896.0	40	0.13	3	1493.38	8	0.34	3	2398.01	7	0.45	3	3091.6	6	0.23	5
907.86[c]	20	0.066	10	1496.80[c]	20	0.061	7	2411.74	15	0.13	1	3112.94[c]	30	0.10	2
920.98	7	0.52	4	1551.7[c]	2	0.061	7	2417.76[c]	15	0.18	2	3132.64	9	0.25	2
940.8	6	0.15	5	1554.58[c]	15	0.11	1	2434.30[c]	15	0.12	1	3142.85	15	0.16	1
944.12	7	1.4	1	1561.01[c]	40	0.0053	20	2446.2	3	0.12	2	3166.81	15	0.31	3
952.66	15	0.74	7	1577.60	7	6.0	4	2451.88	10	0.67	5	3175.74	7	1.30	9
955.14	30	0.36	7	1602.02[c]	40	0.094	20	2454.70	20	0.30	3	3217.61	9	0.33	3
963.92[c]	30	0.074	10	1607.32	7	1.40	9	2462.82	10	0.29	3	3225.90	30	0.11	1
987.79[c]	30	0.048	2	1640.24	20	0.18	3	2469.39[c]	30	0.059	9	3235.50	30	0.13	1
990.34[c]	30	0.013	2	1655.30[c]	40	0.059	10	2498.58	7	0.57	4	3248.45	9	0.40	3
998.56[c]	30	0.042	10	1659.58	9	0.21	2	2509.63	20	0.17	2	3256.92	10	0.32	3
1009.15[c]	30	0.048	10	1685.58	15	0.19	2	2519.05	40	1.30	9	3275.2[c]	2	0.034	4
1017.71[c]	30	0.10	2	1744.3[c]	5	0.069	20	2523.97	10	0.31	3	3281.23	20	0.33	4
1021.26	7	1.30	9	1759.32[c]	15	0.12	1	2536.2[c]	9	0.068	30	3294.1[c]	7	0.043	30
1037.63	7	0.29	2	1768.07	7	0.56	4	2547.12	30	0.38	4	3305.9[c]	5	0.049	20
3314.6	6	0.11	3	3917.06	10	2.0	1	4663.4	4	0.42	4	5195.02	20	0.53	5
3317.8[c]	9	0.058	20	3930.2[c]	10	0.11	5	4669.9	4	0.28	4	5200.84	20	0.55	4

TABLE III. *(continued)*

Energy[a] (keV)		Intensity[b]		Energy[a] (keV)		Intensity[b]		Energy[a] (keV)		Intensity[b]		Energy[a] (keV)		Intensity[b]	
3343.7[c]	5	0.028	5	3970.0[c]	10	0.059	20	4710.23	20	0.39	4	5214.30	30	0.21	2
3361.8	7	0.11	3	4012.34[c]	30	0.0064	8	4728.1	10	0.051	20	5245.4	3	0.18	2
3364.8[c]	7	0.068	20	4027.1	5	0.092	20	4734.44	20	0.24	2	5281.5	9	0.011	4
3381.0	8	0.13	6	4049.95[c]	40	0.10	3	4752.57	20	0.32	3	5318.4[c]	9	0.024	9
3383.3	7	0.15	6	4055.1[c]	8	0.011	4	4770.43	20	0.26	3	5340.0	3	0.14	2
3395.1[c]	7	0.063	2	4092.8[c]	5	0.096	30	4784.32	15	1.8	1	5362.5[c]	12	0.024	10
3435.07	15	0.23	2	4109.86[c]	20	0.10	1	4807.8	4	0.15	2	5369.9	3	0.14	2
3444.77	30	0.10	2	4136.25	40	0.26	8	4824.8	4	0.14	2	5382.9	3	0.15	2
3458.57[c]	30	0.074	9	4180.54	10	4.0	3	4829.8[c]	8	0.0038	10	5395.3[c]	10	0.024	6
3461.06	20	0.28	3	4192.0	10	0.077	20	4836.15	20	0.22	2	5406.16	20	0.21	3
3498.45	30	0.26	3	4204.0	15	0.23	9	4871.90	15	0.45	3	5419.7	5	0.047	15
3536.8[c]	6	0.077	20	4219.1[c]	7	0.096	40	4889.3	5	0.082	20	5424.0	9	0.029	10
3541.79	15	0.44	3	4223.32	30	0.076	8	4917.6	11	0.13	4	5439.7	9	0.010	3
3559.5[c]	6	0.016	5	4231.01[c]	40	0.13	2	4925.6	7	0.18	4	5454.7	3	0.19	2
3598.92	15	0.110	9	4241.66[c]	20	0.050	5	4961.54	15	2.0	1	5473.56	20	0.38	3
3611.87[c]	40	0.097	10	4258.37[c]	30	0.027	3	4975.9	9	0.07	2	5546.5	6	0.033	5
3645.97[c]	20	0.082	8	4265.0	6	0.11	2	5003.0	5	0.054	10	5561.7	9	0.022	7
3657.2	10	0.10	3	4297.18	15	0.53	4	5021.5	3	0.16	3	5594.5	3	0.061	5
3683.2[c]	8	0.057	10	4311.9[c]	10	0.064	20	5033.7	6	0.046	10	5606.2	5	0.049	6
3689.0	5	0.18	4	4326.83	20	0.27	2	5044.54	30	0.44	4	5635.0	5	0.040	5
3693.2[c]	5	0.067	10	4523.96	20	0.29	3	5049.4[c]	22	0.016	10	5648.6	9	0.006	2
3738.2[c]	5	0.074	20	4533.83	30	0.068	7	5059.53	20	0.28	3	5659.7	4	0.027	3
3781.5[c]	7	0.099	30	4539.3[c]	10	0.069	20	5076.08	20	0.19	2	5672.1	4	0.039	4
3794.46	15	0.74	6	4548.16	20	0.120	9	5088.67	40	0.088	10	5685.4	3	0.11	1
3804.6	3	0.17	6	4564.1[c]	5	0.029	6	5103.39	20	0.43	4	5698.6	4	0.018	2
3809.32	15	0.76	6	4572.36	15	0.88	6	5120.23	20	0.53	5	5714.5	9	0.011	2
3829.0[c]	8	0.038	10	4581.9[c]	17	0.11	4	5135.92	20	0.16	2	5793.1	4	0.015	2
3860.90	15	0.26	2	4596.4	6	0.22	6	5154.9	6	0.04	1				
3874.0[c]	8	0.085	20	4620.77	20	0.44	4	5166.6[c]	16	0.016	9				
3909.7	7	0.13	3	4644.58	20	0.82	7	5183.2	3	0.18	2				

[a] In our notation, 93.54 *7* is 93.54 ± 0.07 keV, etc. The γ rays near energies of 611, 854, 1044, 1146, 1356, 1882, 2345, 2639 and 3091 keV are doublets. The energies and intensities of the component γ rays were determined in the $\gamma\gamma$-coincidence measurements.
[b] γ-ray intensity per 100 decays of ^{87}Br. In our notation 0.130 *9* is 0.130 ± 0.009, etc.
[c] γ ray not placed on the level scheme.

nances, while *p*-wave neutrons excite $1/2^-$ or $3/2^-$ resonances. In this experiment, *s*-wave resonances were easily identified from their interference minima (as exemplified in Fig. 4) whenever the widths of the resonances exceeded about 30% of the experimental resolution.

The peak cross section of a resonance can be expressed by $\sigma_0 = 4\pi\lambda\!\!\!^{-2} g\Gamma_n/\Gamma$, which for wide resonances reduces to $\sigma_0 \approx 4\pi\lambda\!\!\!^{-2} g$. The quantity $2\pi\lambda\!\!\!^{-}$ is the de Broglie wavelength in the center of mass system, and the statistical factor g has the value $(2J + 1)/2$ when the target nucleus has zero spin. Here J is the spin of the resonance. Most of the resonances observed in transmission measurements had a width exceeding the experimental resolution. Unambiguous values of g and, consequently, the resonance spins were therefore obtained for all but 9 (out of which 3 are *p* wave) of the observed resonances. For seven of the weakest resonances, one cannot exclude the possibility that some of them represent $3/2^+$ or $5/2^+$ resonances excited by *d*-wave neutrons. This possibility was investigated using the probability arguments developed by Mizumoto *et al.*,[25] who presented the following expression for the probability that a resonance is formed by *d*-wave neutrons:

$$P(d \text{ wave}) = \left\{1 + \frac{3}{5}\left(\frac{S_2P_2}{S_1P_1}\right)^{1/2} \exp\left[\frac{g\Gamma_n}{6\langle D_1\rangle}\sqrt{\frac{1\text{ eV}}{E_n}}\left(\frac{1}{P_2S_2} - \frac{1}{P_1S_1}\right)\right]\right\}^{-1}.$$

TABLE IV. ^{87}Kr coincidence results.

Gating γ ray (keV)	Coincident γ rays (keV)	Gating γ ray (keV)	Coincident γ rays (keV)
230.33	421.74, 1419.71	1443.21	1577.60
263.96	421.74, 1419.71	1449.24	1577.60
421.74	230.33, 263.96, 610.46, 1330.43, 1419.71, 2575.37, 2754.3, 2869.20, 2942.97, 3017.39	1476.06	529.60, 611.5, 823.97, 853.8, 893.42, 896.0, 1311.21, 1356.0, 1360.59, 2169.30, 2398.01, 3048.04, 3804.6
461.52	1419.71		
529.60	831.26, 1021.26, 1476.06, 2704.88	1493.38	1798.31
532.03	944.12, 1349.19, 1768.07, 1840.10, 2693.94, 4533.83, 4663.4, 4669.9, 4770.43	1577.60	681.22, 874.30, 920.98, 1285.66, 1443.21, 1449.24, 1659.58, 2603.20, 3066.85, 3090.8, 3132.64, 3281.23, 3498.45
555.72	3003.91		
610.46	421.74, 1419.71	1607.32	1419.71
611.5	1476.06	1640.24	2005.52
617.49	1349.19, 1881.20	1659.58	1577.60
636.39	2005.52	1685.58	2641.67
651.96	955.14, 1419.71, 2345.3, 2523.97, 2638.7	1768.07	532.03
681.22	1043.3, 1577.60	1798.31	1419.71
698.59	2122.62	1836.78	1419.71
714.09	2122.62	1840.10	532.03, 853.6
724.57	1881.20	1868.72	1419.71
737.96	2519.05	1881.20	617.49, 724.57, 2446.2, 2828.79
823.97	1476.06	1882.2	1419.71
831.26	529.60, 1476.06, 2005.52, 2125.85	1934.67	3026.77
853.6	895.61	1958.23	1476.06
853.8	1476.06, 1840.10	1965.58	421.74, 1419.71
874.30	1577.60	2005.52	636.39, 831.26, 1021.26, 1212.60, 1640.24, 2192.46, 2662.79, 2704.88, 3461.06
893.42	532.03, 944.12, 1476.06		
896.0	1476.06	2071.66	955.14, 1146.23, 2345.3, 2523.97, 2638.7, 2889.8
920.98	1577.60		
940.8	1360.59	2122.62	698.59, 714.09, 1095.16, 3091.6
944.12	532.03, 611.5, 1360.59	2125.85	1360.59, 2836.36
952.66	1419.71	2143.40	2451.88
955.14	651.96, 2071.66	2169.30	1476.06
1021.26	529.60, 2005.52	2192.46	2005.52
1037.63	944.12, 1476.06	2226.11	1419.71
1043.3	681.22	2299.93	3166.81
1044.3	3917.06	2345.3	651.96, 2071.66
1078.88	1419.71	2345.4	1577.60
1095.16	2122.62	2369.39	none
1099.88	1355.1, 1419.71	2372.38	853.8
1146.23	1419.71	2398.01	1476.06
1186.27	421.74?, 1419.71?	2411.74	2005.52
1212.60	529.60, 1476.06, 2005.52	2446.2	1881.20
1285.66	1577.60	2451.88	2509.63
1291.7	529.60, 2005.52	2454.70	1419.71
1311.21	1476.06	2462.82	none
1330.43	421.74, 1419.71	2498.58	none
1338.03	1419.71	2509.63	2451.88
1344.60	1360.59, 1476.06, 2836.36	2519.05	737.96, 1126.78, 1355.1
1349.19	532.03	2523.97	651.96, 2071.66
1355.1	2519.05	2575.37	421.74, 1419.71
1356.0	1476.06	2603.20	1577.60
1360.59	940.8, 944.12, 1344.60, 1476.06, 2125.85	2638.7	651.96, 2071.66
1376.08	421.74, 1419.71	2639.0	2641.67
1389.77	1360.59	2641.67	1685.58, 2639.0
1415.43	421.74, 1419.71	2662.79	2005.52
1419.71	421.74, 461.52, 651.96, 952.66, 1078.88, 1099.88, 1338.03, 1607.32, 1798.31, 1836.78, 1868.72, 1882.2, 2226.11, 2454.70, 2907.46, 2997.21, 3175.74, 3235.50, 3248.45, 3541.79, 3794.46, 3860.90	2693.94	532.03
		2704.88	529.60, 2005.52
		2715.19	none
		2754.3	421.74, 1419.71

TABLE IV. *(continued)*

Gating γ ray (keV)	Coincident γ rays (keV)	Gating γ ray (keV)	Coincident γ rays (keV)	Gating γ ray (keV)	Coincident γ rays (keV)
2820.97	none	3598.92	none	4836.15	none
2828.79	1881.20	3657.2	none	4871.90	none
2836.36	2125.85	3689.0	none	4889.3	none
2869.20	421.74, 1419.71	3794.46	1419.71	4917.6	none
2889.8	2071.66	3804.6	1476.06	4925.6	none
2907.46	1419.71	3809.32	none	4961.54	none
2942.97	421.74, 1419.71	3860.90	1419.71	4975.9	none
2997.21	1419.71	3909.7	none	5003.0	none
3003.91	555.72	3917.06	1044.3	5021.5	none
3017.39	421.74, 1419.71	4027.1	none	5033.7	none
3026.77	1934.67	4136.25	none	5044.54	none
3048.04	1476.06	4180.54	none	5059.53	none
3066.85	1577.60	4192.0	none	5076.08	none
3080.72	none	4204.0	none	5088.67	none
3090.8	1577.60	4223.32	none	5103.39	none
3091.6	2122.62	4265.0	none	5120.23	none
3132.64	1577.60	4297.18	none	5135.92	none
3142.85	none	4326.83	none	5154.9	none
3166.81	2299.93	4523.96	none	5183.2	none
3175.74	1419.71	4533.83	532.03	5195.02	none
3217.61	none	4548.16	none	5200.84	none
3225.90	none	4572.36	none	5214.30	none
3235.5	1419.71	4596.4	none	5245.4	none
3248.45	1419.71	4620.77	none	5340.0	none
3256.92	none	4644.58	none	5369.9	none
3281.23	1577.60	4663.4	532.03	5382.9	none
3314.6	1419.71	4669.9	532.03	5406.16	none
3361.8	none	4710.23	none	5419.7	none
3381.0	611.5	4728.1	none	5454.7	none
3383.3	1577.60	4734.44	none	5473.56	none
3435.07	none	4752.57	none	5606.2	none
3444.77	none	4770.43	532.03	5635.0	none
3461.06	2005.52	4784.32	none	5659.7	none
3498.45	1577.60	4807.8	none	5672.1	none
3541.79	1419.71	4824.8	none	5685.4	none

The quantity E_n is the resonance energy in eV, S_1 and S_2 are the p-wave and d-wave strength functions, and P_1 and P_2 are the penetrabilities for $l = 1$ and 2. The average spacing of $l = 1$ resonances is denoted by D_1 and has been taken to be $\approx$12 keV from the present data. The d-wave strength function S_2 was assumed to have the same magnitude as S_0, which is derived below. A nuclear radius of 5.98 fm was used for the calculation of the penetrabilities. The resulting values of P (d wave) derived for weak resonances (see Table VII) showed that four of these may have a probability of greater than 50% for being formed by d-wave interaction. Because of the weakness of these resonances, a possible d-wave assignment for some of them will not significantly influence the strength functions discussed below. The p-wave level density should not be affected by more than $\approx$10%. The main point where the actual number of d-wave resonances at low energies is of interest is in the comparison between the neutron resonance and the β-decay results (see Sec. III C below). It should be emphasized that rather large uncertainties are associated with the P (d wave) values because they depend on the rather uncertain strength functions S_1 and S_2.

A final remark concerning the majority of the resonances for which definite l values were deduced is that the spin and parity assignments thus made (see Tables I and II) for a number of unbound levels in ^{87}Kr can be considered to be firm. As will be discussed, they also lead to a unique J^π assignment for the β-decaying ground state of ^{87}Br.

B. Level density and neutron strength functions

The total cross-section measurements have been analyzed up to a maximum energy of 400 keV. The

TABLE V. ^{87}Kr level scheme in tabular form.

Level energy[a] (keV)		De-exciting γ rays[b]	Level energy[a] (keV)		De-exciting γ rays[b]
0.0			3909.8	7	3909.7
531.99	4	532.03	3917.16	10	3917.06
1419.65	3	1419.71	3923.0	6	2345.4
1476.12	4	944.12, 1476.06	4027.2	5	4027.1
1577.59	4	1577.60	4136.4	5	4136.25
1841.41	5	421.74	4180.82	6	1344.60, 2603.20, 4180.54
1881.19	5	461.52, 1349.19, 1881.20	4192.1	10	4192.0
2005.42	3	529.60, 2005.52	4197.91	11	2192.46
2071.64	4	230.33, 651.96, 2071.66	4204.1	15	4204.0
2086.7	6	611.5	4223.43	30	4223.32
2105.37	8	263.96	4226.33	8	1389.77
2122.53	5	2122.62	4265.1	6	4265.0
2258.68	7	681.22, 2258.44	4297.29	15	4297.18
2300.02	6	823.97, 1768.07, 2299.93	4327.20	9	1685.58, 2446.2, 2907.46, 4326.83
2329.9	6	853.8	4416.92	6	2345.3, 2411.74, 2575.37, 2997.21
2369.49	7	893.42, 2369.39	4524.15	14	3048.04, 4523.96
2372.35	6	896.0, 952.66, 1840.10, 2372.38	4548.29	20	4548.16
2451.90	5	610.46, 874.30, 2451.88	4572.49	15	4572.36
2462.86	10	2462.82	4595.50	6	2143.40, 2523.97, 2754.3, 3175.74, 4596.4
2498.58	5	617.49, 920.98, 1078.88, 2498.58	4620.90	20	4620.77
2513.76	8	1037.63	4644.57	12	3066.85, 4644.58
2519.01	7	1099.88, 2519.05	4655.21	30	3235.50
2547.2	4	2547.12	4668.19	8	2662.79, 3090.8, 3248.45
2565.9	6	1146.2	4710.34	5	2638.7, 2704.88, 2828.79, 2869.20, 3132.64, 4710.23
2605.77	16	724.57			
2641.74	6	636.39, 2641.67	4711.25	9	1493.38
2715.24	10	2715.19	4728.2	10	4728.1
2757.69	8	1338.03	4734.55	19	3314.6, 4734.44
2787.34	11	1311.21	4752.71	20	4752.57
2821.06	6	698.59, 2820.97	4784.46	13	2942.97, 4784.32
2832.1	6	1356.0	4807.9	5	4807.8
2836.55	4	714.09, 831.26, 1360.59, 2836.36	4824.9	5	4824.8
2863.26	10	1285.66	4836.29	20	4836.15
3003.97	30	3003.91	4858.87	13	3017.39, 3281.23
3020.81	15	1443.21	4872.05	15	4871.90
3026.84	4	955.14, 1021.26, 1449.24, 1607.32, 3026.77	4889.4	6	4889.3
3080.78	15	3080.72	4917.7	11	4917.6
3142.91	15	3142.85	4925.8	8	4925.6
3171.85	16	1330.43	4961.55	6	1044.3, 1934.67, 2509.63, 2889.8, 3383.3, 3541.79, 4961.54
3217.86	5	1095.16, 1146.3, 1212.60, 1376.08, 1798.31, 3217.61			
			4962.43	20	2125.85
3225.97	10	853.6, 2693.94, 3225.90	4976.0	10	4975.9
3237.18	10	1659.58	5003.2	6	5003.0
3256.77	5	737.96, 1415.43, 1836.78, 3256.92	5021.7	4	5021.5
3288.39	30	1868.72	5033.9	7	5033.7
3297.13	20	1291.7	5044.7	3	5044.54
3301.9	4	1043.3, 1882.2	5059.69	20	5059.53
3361.9	7	3361.8	5065.95	30	4533.83
3434.76	11	1958.23, 3435.07	5076.20	20	3498.45, 5076.08
3444.8 ?	4	3444.77	5088.8	5	5088.67
3559.7	4	555.72	5103.55	20	5103.39
3599.00	20	3598.92	5120.39	20	5120.23
3645.54	7	1126.78, 1640.24, 2169.30, 2226.11	5136.08	20	5135.92
3657.3	10	3657.2	5155.1	7	5154.9
3689.1	6	3689.0	5183.37	30	5183.2
3777.4	7	940.8	5195.25	18	4663.4, 5195.02
3807.01	10	1965.58	5201.21	18	4669.9, 5200.84
3809.41	15	3809.32	5214.25	13	3091.6, 3794.46, 5214.30
3874.19	8	1355.1, 2398.01, 2454.70			
5245.6	4	5245.4	5546.7	6	5546.5

TABLE V. *(continued)*

Level energy[a] (keV)		De-exciting γ rays[b]	Level energy[a] (keV)		De-exciting γ rays[b]
5280.70	*14*	2639.0, 3804.6, 3860.90, 5281.5	5561.9	*9*	5561.7
5302.56	*20*	4770.43	5594.7	*3*	5594.5
5340.18	*30*	5340.0	5606.4	*5*	5606.2
5370.08	*30*	5369.9	5635.2	*5*	5635.0
5383.08	*30*	5382.9	5648.8	*9*	5648.6
5406.34	*20*	5406.16	5659.9	*4*	5659.7
5419.9	*5*	5419.7	5672.3	*4*	5672.1
5424.2	*9*	5424.0	5685.6	*3*	5685.4
5439.9	*9*	5439.7	5698.8	*4*	5698.6
5454.9	*3*	5454.7	5714.7	*9*	5714.5
5466.79	*13*	3166.81, 3381.0, 3461.06	5793.3	*4*	5793.1
5473.74	*20*	5473.56			

[a] In our notation 531.99 *4* is 531.99 ± 0.04 keV, etc.
[b] See Table III for the appropriate absolute photon intensity.

corresponding excitation energy in ^{87}Kr spans the region from 5.515 to 5.915 MeV. A total of 41 resonances were seen, of which 10 and 25 could be definitely assigned as being s wave and p wave, respectively. Assuming that the reduced widths of the resonances follow a Porter-Thomas distribution, one can use the known sensitivity of the experiment to estimate[26] that about six resonances were not observed in the present experiment. The six unobserved resonances, together with the six unassigned resonances, can be distributed over different spins and parities with the same frequencies as found for firmly assigned resonances, thus yielding total expected numbers of 13, 11, and 23 for $s_{1/2}$, $p_{1/2}$, and $p_{3/2}$ resonances, respectively. In the terminology of the Fermi-gas level-density formula with a conventionally chosen value of the spin cutoff factor (see e.g., Ref. 2), these numbers correspond to values of the level density parameter of 9.8 and 9.7 MeV^{-1} for positive parity and negative parity levels, respectively. The latter value can be used to estimate the expected number of $5/2^-$ levels in the region studied to be 26. These levels are most probably not seen in the total cross-section measurements (see Sec. III C below) but are of importance because they may be populated in the β decay of ^{87}Br. It is of interest to note that the value of the level density parameter for ^{87}Kr found currently (9.7 MeV^{-1}) is considerably smaller than the one inferred ($\approx$13 MeV^{-1}) from a theoretical simulation[2] of the delayed neutron spectrum.

The Fermi-gas model assumes an equal number of levels of both parities for each spin value. The present results for ^{87}Kr support this assumption in the region of excitation energy studied here.

The neutron strength functions are important because they can be used for the calculation of average cross sections in the unresolved region. For a given partial wave, the definition of the strength function is $S_l = [1/(2l + 1)]\Sigma g\Gamma^l/\Delta E$, where ΔE is the energy interval studied. For ^{87}Kr, the present data yield $S_0 = (0.9 \pm 0.4) \times 10^{-4}$ and $S_1 = (3.2 \pm 0.9) \times 10^{-4}$. These values are similar to what have been found[27] for other nuclei in the $A = 90$ region. The large uncertainty in S_0 is a consequence of the small number of s-wave resonances that were observed. Only resonances with well-established l values were included in the derivation of S_0 and S_1. The omission of the few weak unassigned or unobserved resonances will not significantly affect these values.

The reduced neutron widths given in Tables I and II for p-wave resonances exhibit a strong correlation between large reduced widths and $J = 3/2$. Figure 6 shows staircase plots of the reduced neutron widths for both $1/2^-$ and $3/2^-$ resonances. The observed ratio of the cumulative widths of $3/2^-$ to $1/2^-$ is about 7, whereas the simple statistical value for this ratio is 2. Many years ago, Fiedeldey and Frahn[28] presented a theoretical model with a splitting of the p-wave strength function into $p_{1/2}$ and $p_{3/2}$ components due to the spin-orbit coupling term in the optical potential. Their results predict that, for $A = 87$, the $p_{3/2}$ strength should be significantly larger than the $p_{1/2}$ strength.

Using the compilation for other nuclei given by Mughabghab, Divadeenam, and Holden,[27] additional evidence was sought to support the splitting of the p-wave strength function. The results of this

Table VI. Decay of ^{87}Kr.

Level energy (keV)		% β^-	Log ft	Level energy (keV)		%β^-	Log ft	Level energy (keV)		% β^-	Log ft
0.0	0	12.1	7.38	3434.76	11	0.39	7.51	4925.8	8	0.18	6.79
531.99	4	1.2	8.22	3444.8	4	0.10	8.10	4961.55	6	3.1	5.52
1419.65	3	4.8	7.32	3559.7	4	0.047	8.36	4962.43	20	0.19	6.73
1476.12	4	1.7	7.75	3599.00	20	0.11	7.97	4976.0	10	0.07	7.15
1577.59	4	1.3	7.83	3645.54	7	0.96	7.00	5003.2	6	0.05	7.27
1841.41	5	<0.5	> 8.1	3657.3	10	0.10	7.98	5021.7	4	0.16	6.75
1881.19	5	2.3	7.47	3689.1	6	0.18	7.70	5033.9	7	0.05	7.24
2005.42	3	<1.1	> 7.7	3777.4	7	0.15	7.73	5044.7	3	0.44	6.29
2071.64	4	2.2	7.41	3807.01	10	0.22	7.54	5059.69	20	0.28	6.47
2086.7	6	<0.2	> 8.4	3809.41	15	0.76	7.00	5065.95	30	0.068	7.08
2105.37	8	0.20	8.44	3874.19	8	0.85	6.91	5076.20	20	0.45	6.25
2122.53	5	0.55	7.99	3909.8	7	0.13	7.71	5088.8	5	0.09	6.93
2258.68	7	0.41	8.06	3917.16	10	1.94	6.53	5103.55	20	0.43	6.24
2300.02	6	0.68	7.82	3923.0	6	0.12	7.73	5120.39	20	0.53	6.13
2329.9	6	<0.07	> 8.7	4027.2	5	0.09	7.79	5136.08	20	0.16	6.63
2369.49	7	0.96	7.64	4136.4	5	0.26	7.26	5155.1	7	0.04	7.22
2372.35	6	2.2	7.28	4180.82	6	4.6	5.98	5183.37	30	0.18	6.53
2451.90	5	1.24	7.50	4192.1	10	0.08	7.73	5195.25	18	0.95	5.80
2462.86	10	0.29	8.12	4197.91	11	0.31	7.14	5201.21	18	0.83	5.85
2498.58	5	1.31	7.45	4204.1	15	0.23	7.26	5214.25	13	1.18	5.68
2513.76	8	0.29	8.10	4223.43	30	0.08	7.71	5245.6	4	0.18	6.47
2519.01	7	0.74	7.69	4226.33	8	0.11	7.57	5280.70	14	0.56	5.93
2547.2	4	0.38	7.97	4265.1	6	0.11	7.54	5302.56	20	0.26	6.24
2565.9	6	0.16	8.33	4297.29	15	0.53	6.83	5340.18	30	0.14	6.47
2605.77	16	0.08	8.62	4327.20	9	0.98	6.55	5370.08	30	0.14	6.43
2641.74	6	0.44	7.86	4416.92	6	3.4	5.94	5383.08	30	0.15	6.39
2715.24	10	0.19	8.19	4524.15	14	0.39	6.80	5406.34	20	0.21	6.22
2757.69	8	0.74	7.58	4548.29	20	0.12	7.29	5419.9	5	0.05	6.35
2787.34	11	0.16	8.23	4572.49	15	0.88	6.40	5424.2	9	0.03	7.04
2821.06	6	1.94	7.11	4595.50	6	2.3	5.97	5439.9	9	0.010	7.50
2832.1	6	0.07	8.57	4620.90	20	0.44	6.67	5454.9	3	0.19	6.20
2836.55	4	5.6	6.66	4644.57	12	0.95	6.31	5466.79	13	0.72	5.61
2863.26	10	0.22	8.06	4655.21	30	0.13	7.17	5473.74	20	0.38	5.87
3003.97	30	0.07	8.49	4668.19	8	0.83	6.35	5546.7	6	0.033	6.84
3020.81	15	0.14	8.18	4710.34	5	3.2	5.73	5561.9	9	0.022	7.00
3026.84	4	5.2	6.60	4711.25	9	0.34	6.70	5594.7	3	0.061	6.51
3080.78	15	0.17	8.06	4728.2	10	0.05	7.52	5606.4	5	0.049	6.59
3142.91	15	0.16	8.06	4734.55	19	0.35	6.67	5635.2	5	0.040	6.64
3171.85	16	0.14	8.10	4752.71	20	0.32	6.69	5648.8	9	0.006	7.44
3217.86	5	1.12	7.17	4784.46	13	1.88	5.90	5659.9	4	0.027	6.77
3225.97	10	0.62	7.42	4807.9	5	0.15	6.97	5672.3	4	0.039	6.60
3237.18	10	0.21	7.89	4824.9	5	0.14	6.99	5685.6	3	0.11	6.13
3256.77	5	3.7	6.63	4836.29	20	0.22	6.78	5698.8	4	0.018	6.89
3288.39	30	0.13	8.07	4858.87	13	0.60	6.33	5714.7	9	0.011	7.08
3297.13	20	0.11	8.14	4872.05	15	0.45	6.44	5793.3	4	0.015	6.83
3301.9	4	0.72	7.32	4889.4	6	0.08	7.17				
3361.9	7	0.11	8.10	4917.7	11	0.13	6.94				

survey were somewhat inconclusive. The cumulative p-wave strengths for ^{64}Zn, ^{92}Zr, ^{94}Zr, and ^{98}Mo did indicate an enhanced $p_{3/2}$ strength. On the other hand, the results for ^{68}Zn, ^{88}Sr, ^{90}Zr, and ^{92}Mo did not show evidence for enhanced $p_{3/2}$ over $p_{1/2}$ strength.

C. Overlap between β decay and resonance neutron spectroscopy

The $1/2^+$ levels in ^{87}Kr observed as s-wave resonances and possible $3/2^+$ or $5/2^+$ levels observed as d-wave resonances will be disregarded in the

TABLE VII. Probability test for *d*-wave assignments of weak resonances.

E_n[a] (keV)	$g\Gamma_n$ (eV)	$P(d\text{-wave})$[b] %	$P(p\text{-wave})$[c] %
5.609	0.024	37	63
11.629	0.026	96	4
25.829	1.5	$<10^{-1}$	>99.9
48.659	2.1	80	20
68.613	25	$<10^{-3}$	>99.9
79.392	9.8	59	41
88.270	≈4	≈90	≈10

[a]See also Table I. An *s*-wave assignment can be ruled out only for the 68.613 keV resonance.
[b]See formula given in Sec. III A.
[c]$P(p\text{-wave}) = 100 - P(d\text{-wave})$.

following discussions. The reason is that such levels may be populated only by first-forbidden β transitions, which in general are one or two orders of magnitude weaker than the allowed ones. This degree of retardation is not confirmed for first-forbidden transitions to levels at relatively high excitation energy such as those of interest here. It would nevertheless be surprising if a first-forbidden transition could have sufficient intensity to produce a detectable peak in the delayed neutron spectrum of Nuh *et al.*,[1] and no evidence was found for this.

It also appears that none of the 12 unbound levels observed in the Ge(Li) γ-ray decay scheme study (see Table V) can be identified with the *p*-wave resonances found currently. Eleven of these levels are relatively evenly distributed over the first 200 keV above the binding energy, and the remaining one is found at 277.9 keV. The uncertainties in the measured values for the γ-ray energies and the binding energy (5515.4 ± 0.8 keV) allow some of the levels to agree in energy with some of the *p*-wave resonances. Considerations based on the expected magnitudes of Γ_γ and the measured values of Γ_n for these resonances, combined with the observed intensities of the γ rays, show that unreasonably high delayed neutron intensities would result, in contradiction with the measurements, if these levels are identified with these resonances on the basis of nearly matching energies. Instead, one can safely assign the γ-decaying levels as $5/2^-$, which requires *f*-wave neutron emission and, consequently, much lower Γ_n at low energies. The average Γ_n for *f*-wave neutrons can be estimated reasonably well (see Fig. 7). The neutron

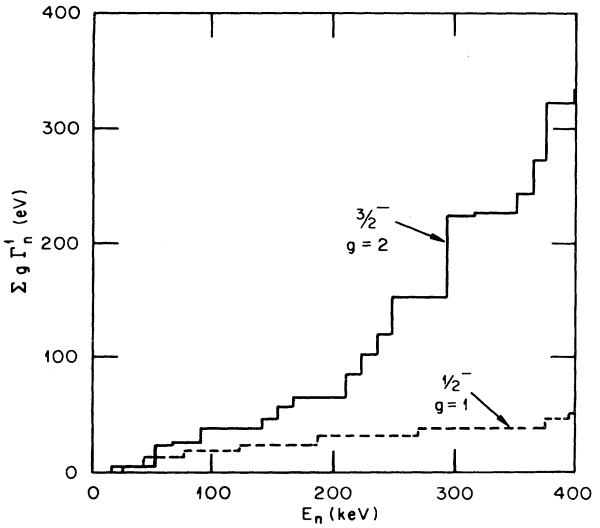

FIG. 6. Plots of the sum of reduced neutron widths for $p_{3/2}$ and $p_{1/2}$ resonances vs neutron energy. In making these plots, the 19.2- and 68.6-keV resonances (see Table I) were assumed as $3/2^-$, and the 27.8-keV resonance was assumed as $1/2^-$. The observed ratio of the cumulative widths is about 7 for $3/2^-$ to $1/2^-$, whereas a simple statistical estimate for this ratio is 2.

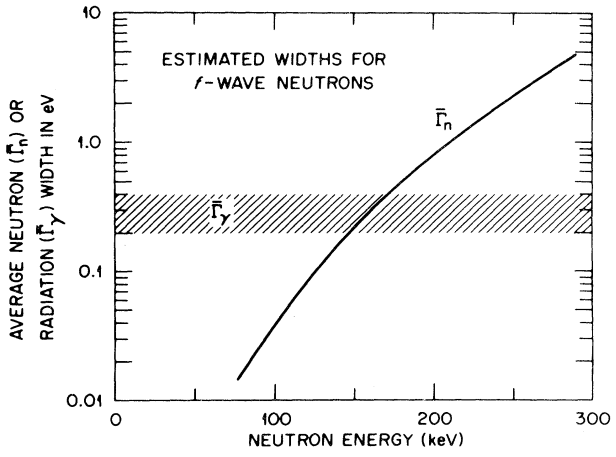

FIG. 7. The expected average neutron width for *f*-wave neutron emission from $5/2^-$ levels has been estimated as shown by the full line from the observed (smoothed) average width of *p*-wave resonances and the ratio of the penetrabilities for *f* and *p* waves. A nuclear radius of 5.98 fm was used. The hatched area represents the most likely values for the 0 radiation widths. The influence of the statistical factor, *g*, has been disregarded in the estimates shown.

widths are expected to follow a Porter-Thomas distribution so that only a small fraction of the widths have values a few times higher than the average. It is therefore probable that no $5/2^-$ levels in ^{87}Kr at energies below $S_n + \approx 200$ keV have neutron widths sufficiently large to be seen either in the delayed neutron spectrum of Ref. 1 or in the present transmission measurements. Conversely, it can be inferred that no $5/2^-$ levels situated well above this energy are likely to decay by detectable γ rays.

Because s-wave and d-wave neutrons have been previously excluded, the conclusion is drawn that only p-wave neutrons will contribute to the region below 200–250 keV in the delayed neutron spectrum of Ref. 1. It is also concluded that a clean separation exists between the unbound levels seen in Ge(Li) γ-ray studies on the one hand and those seen in delayed neutron emission studies on the other.

A detailed comparison of the low-energy part of the delayed neutron spectrum with the presently obtained p-wave resonance data is also carried out in Table VIII. The agreement is good, thus showing almost a one-to-one correspondence between delayed neutron lines and p-wave neutron resonances up to about 200 keV. This good agreement also shows that the decomposition of the delayed neutron spectrum presented in Ref. 1 is certainly meaningful and that delayed neutron spectroscopy can indeed be used to study the decay of individual levels in a relatively heavy nucleus such as ^{87}Kr. The agreement is all the more remarkable because the decomposition was made several years ago without the benefit of the high-resolution data provided by the present complementary measurements of neutron resonance reactions. The rapidly increasing widths of $1/2^-$ and $3/2^-$ levels, in combination with the onset of f-wave neutron emission from $5/2^-$ levels, will however most probably prohibit a meaningful decomposition of the delayed neutron spectrum for energies well above 200–250 keV. Nevertheless, because the locations of neutron resonances are now accurately known, the delayed neutron spectrum presented in Ref. 1 was reanalyzed up to 400 keV in order to extract better intensity values. These results are included in Table VIII.

There are delayed neutron groups associated with both $p_{1/2}$ and $p_{3/2}$ resonances showing that unbound levels with both spin values are populated in the β decay. The observed γ-decaying unbound levels discussed earlier all have $J^\pi = 5/2^-$. The spin and parity of the β-decaying ground state of ^{87}Br are thus most probably $3/2^-$.

D. Selectivity of β decay

With available knowledge, it is possible also to discuss nuclear-structure-dependent selectivity of the β decay of ^{87}Br. Such a selectivity would have the consequence that only a small proportion of the levels are strongly populated, the result of which should give a marked deviation of the distribution of the β feeding of the levels from a Porter-Thomas distribution.

The intensities and log ft values for about 160 β branches are given in Tables VI and VIII. For Gamow-Teller (G-T) β transitions, the matrix elements are given by[29]

$$<\sigma\tau>^2 = K/(G_A^2\, ft) ,$$

where $K = 1.23 \times 10^{-94}$ erg^2 cm^6 s and G_A is the renormalized axial-vector coupling constant. The use of the free neutron value,[30] $G_A = 1.78 \times 10^{-49}$ erg cm^3, implies neglecting any renormalization in the nuclear medium. The relative G-T matrix elements, deduced from the above expression and the log ft values, are shown in Fig. 8. (The implicit assumption has been made here that all β transitions are of the allowed Gamow-Teller type.)

Above 400 keV (5915 keV excitation energy), a peak analysis of the delayed neutron spectrum is not meaningful. Therefore, for the purpose of extracting the G-T matrix elements just below Q_β, the neutron spectrum was treated as a continuum divided into 20-keV (which roughly corresponds to the detector resolution in this energy region) intervals. The matrix elements, which thus extended from 5915 keV to 6805 keV, are also shown in Fig. 8. The overall β-strength distribution is dominated by a resonance centered at about 5.3 MeV and by the rising tail of a second resonance situated above Q_β. The distribution is certainly not a smoothly increasing function as predicted by statistical models. (The structures are by no means washed out by binning the matrix elements into, say, 100 keV bin widths.) The observed features can be reproduced however by both random phase approximation (RPA) and shell model + pairing calculations.[31] They predict concentrations of strengths near 5 and 7 MeV arising from transitions involving the $\nu p_{1/2}$-$\pi p_{3/2}$ "back spin flip" and the $\nu p_{3/2}$-$\pi p_{3/2}$ "core polarized" configurations,

Table VIII. Unbound levels in ^{87}Kr listed as E_x (excitation energy in keV) and as $E_x - S_n$ (neutron separation energy, 5515.4 ± 0.8 keV) together with β-decay properties.

Present work[a] ^{87}Br decay delayed γ rays $(E_x - S_n)$ (keV)		J^π [b]	Nuh *et al.*[c] ^{87}Br decay delayed neutrons $(E_x - S_n)$ (keV)		Present work ^{86}Kr+n resonances[d] $(E_x - S_n)$ (keV)	J^π [e]	E_x (keV)		$\%\beta^-$ [f]		$\%\beta^-$ [g]	Log ft
					5.54	$1/2^\pm,3/2^\pm,5/2^+$	5520.9	*9*				
					11.49	$1/2^\pm,3/2^\pm,5/2^+$	5526.9	*9*				
			18.2	*15*	19.01	$1/2^-,3/2^-$	5534.4	*9*	0.36	*4*		5.82
					25.53	$1/2^\pm,3/2^-$	5540.9	*9*	0.036	*29*		6.8
					27.52	$1/2^-,3/2^-$	5542.9	*9*				
31.3	*14*	$(5/2^-)$					5546.7	*6*			0.033	6.84
			40.8	*15*	43.41	$1/2^-$	5558.8	*9*	0.065	*7*		6.53
46.5	*17*	$(5/2^-)$					5561.9	*9*			0.022	7.00
					48.10	$1/2^\pm,3/2^\pm,5/2^+$	5563.5	*9*				7.00
			52.8	*23*	53.75	$3/2^-$	5569.2	*9*	0.287	*25*		5.87
			71.6	*17*	67.82	$1/2^-,3/2^-$	5583.2	*9*	0.133	*25*		6.19
			80.8	*26*	77.96	$1/2^-$	5593.4	*9*	0.093	*25*		6.33
					78.48	$1/2^\pm,3/2^\pm,5/2^+$	5593.9	*9*				
79.3	*11*	$(5/2^-)$					5594.7	*3*			0.061	6.51
					87.26	$1/2^\pm,3/2^\pm,5/2^+$	5602.7	*9*				
91.0	*13*	$(5/2^-)$					5606.4	*5*			0.049	6.59
					91.05	$3/2^-$	5606.5	*9*	<0.018			>7.0
119.8	*13*	$(5/2^-)$					5635.2	*5*			0.040	6.64
			122.5	*28*	123.10	$1/2^-$	5638.5	*9*	0.126	*14*		6.13
133.4	*17*	$(5/2^-)$					5648.8	*9*			0.006	7.44
			137.4	*19*	140.44	$3/2^-$	5655.8	*9*	0.129	*14*		6.10
144.5	*12*	$(5/2^-)$					5659.9	*4*			0.027	6.77
			149.2	*25*	155.05	$3/2^-$	5670.4	*9*	0.104	*14*		6.17
156.9	*12*	$(5/2^-)$					5672.3	*4*			0.039	6.60
			171.2	*32*	167.42	$3/2^-$	5682.8	*9*	0.057	*18*		6.42
170.2	*11*	$(5/2^-)$					5685.6	*3*			0.11	6.13
183.4	*12*	$(5/2^-)$					5698.8	*4*			0.018	6.89
			183.9	*32*	186.38	$1/2^-$	5701.8	*9*	0.151	*18*		5.97
199.3	*17*	$(5/2^-)$					5714.7	*9*			0.011	7.08
			213.6	*24*	209.02	$3/2^-$	5724.2	*9*	0.047	*18*		6.4
					220.95	$3/2^-$	5736.4	*9*	0.050	*18*		6.39
					234.86	$3/2^-$	5750.3	*9*	<0.018			>6.8
			250.9	*35*	245.73	$3/2^-$	5761.1	*9*	0.180	*25*		5.80
			259.2	*25*	266.97	$1/2^-$	5782.4	*9*	0.057	*28*		6.3
277.9	*12*	$(5/2^-)$					5793.3	*4*			0.015	6.83
					289.95	$3/2^-$	5805.4	*9*	<0.018			>6.7
			316.0	*24*	312.72	$3/2^-$	5828.1	*9*	0.047	*11*		6.28
			343.2	*31*	346.42	$3/2^-$	5861.8	*9*	0.022	*11*		6.6
					358.70	$3/2^-$	5874.1	*9*	<0.011			>7.0
					368.74	$3/2^-$	5884.1	*9*	<0.011			>7.0
					370.35	$1/2^-$	5885.8	*9*	<0.011			>7.0
					387.78	$1/2^-$	5903.2	*9*	0.029	*8*		6.4
			390.8	*32*	392.33	$3/2^-$	5907.7	*9*				
			406,	etc.								

TABLE VIII. *(continued)*

[a]In our notation, 31.3 *14* ≡ 31.3 ± 1.4 keV, etc. The quoted uncertainties include the uncertainty in S_n.
[b]An open γ-ray channel here implies a blocked neutron channel, e.g., *f*-wave neutron emission.
[c]Reference 1. In our notation, 18.2 *15* ≡ 18.2 ± 1.5 keV, etc.
[d]Resonance energy corrected for recoil.
[e]Definite *s*-wave resonances are excluded in this table. See also Tables I and II.
[f]Reanalysis of the delayed neutron spectrum presented in Ref. 1. The peaks in the 10-350 keV neutron energy region account for 90% of the total neutron emission probability of (2.48 ± 0.11)%. This probability is an average value recommended by G. Rudstam, *Proceedings of the Consultants' Meeting on Delayed Neutron Properties,* INDC (NDS) 107G + Special (IAEA, Vienna 1979) p. 69.
[g]Since these values are based on the intensities of the γ rays observed to decay only to the ^{87}Kr ground state, they represent lower limits. The corresponding log *ft* values are upper limits.

respectively. (The terminology used here is defined, for example, in Refs. 32 and 33.)

Even though broad structures are visible in Fig. 8, the β decay to individual levels in the unbound region of ^{87}Kr does not appear to be very selective because delayed neutron groups are associated with almost all the $1/2^-$ and $3/2^-$ levels observed in the neutron resonance measurements. Following the maximum likelihood method as outlined by Lynn,[34] a χ^2 distribution with an arbitrary number of degrees of freedom was fitted to the set of G-T matrix elements (reduced β-transition probabilities) in the 5.52–5.73 MeV excitation energy region (see Table VIII). The 13 definite $1/2^-$ or $3/2^-$ levels in this region yielded a rather imprecise result that allowed up to 4 degrees of freedom. The main cause of this uncertainty is the poorly known number of $1/2^-$ or $3/2^-$ levels present in this region. If the number of levels used in the fitting procedure is increased to 19 (which is permitted by the present data), the number of degrees of freedom drops quickly to about 2. In analyzing the earlier data for a wider (4.67–5.90 MeV) energy region, Nuh *et al.*[1] have already shown that the fluctuations in the β-transition probabilities for 31 transitions are quite well described by a Porter-Thomas distribution.

The same conclusion applies to the $5/2^-$ levels observed in the γ-ray study because the level-density parameter derived in Sec. III suggests that about 13 levels with $J^\pi = 5/2^-$ should be present in the region up to about 200 keV above the bind-

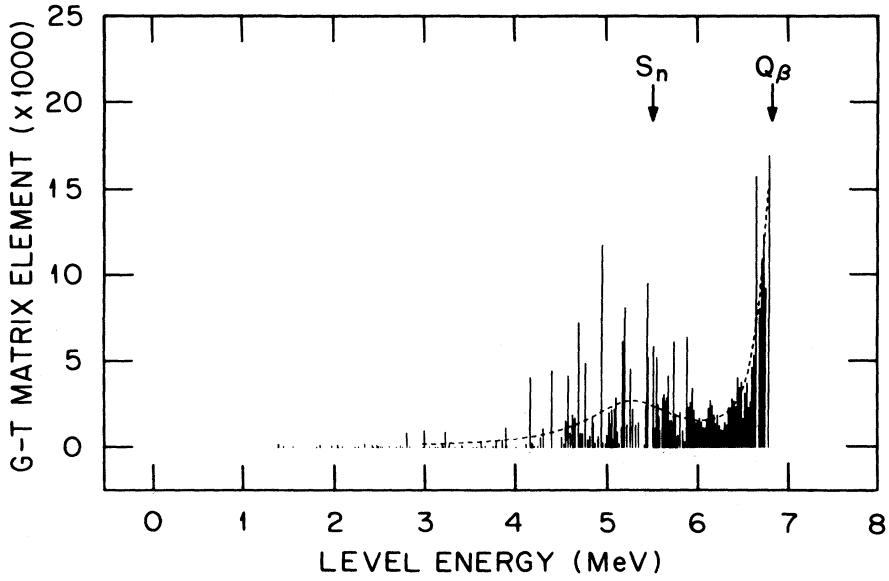

FIG. 8. Gamow-Teller matrix elements (reduced transition probabilities) for β^- decay of ^{87}Br to levels in ^{87}Kr deduced from γ-ray and delayed neutron measurements. The Lorentzian fits (dashed line) are mainly to guide the eye.

ing energy. Experimentally, the γ-ray decay scheme shows 11 such levels, a finding which again implies that no marked selectivity is present.

The more than 200 matrix elements shown in Fig. 8 render ^{87}Br decay one of the best studied decays throughout the periodic table. The sum of the matrix elements (=0.353) represents 0.7% of the (nearly) model independent G-T sum rule strength [given by[35] $\approx 3(N - Z)$] of 51. By comparison, the shell model + pairing calculation[31] predict a sum rule strength of 52.1, thus implying negligible Pauli blocking.

E. Stellar average neutron capture cross section

Despite its substantial yield as a fission product, ^{86}Kr is not of concern as a significant fission product poison in reactor fuel because of its very small neutron capture cross section. It is of concern in astrophysical nucleosynthesis, where neutron capture by ^{85}Kr can produce ^{86}Kr much more rapidly than ^{86}Kr is transmuted to ^{87}Kr.

Models of stellar interior regions where nucleosynthesis can occur imply neutron energies in thermal equilibrium at temperatures in the neighborhood of $kT = 30$ keV, where k is the Boltzmann constant. Theoretical estimates of the ^{86}Kr(n,γ) average capture rate [see Ref. 36 for definition (especially the units)], relying on average nuclear properties, give 9 mb (Ref. 36), 4.4 mb (Ref. 37), and 3.7 mb (Ref. 38) for this rate. Because the s-wave average level spacing is about 40 keV (see Tables I and II), the detailed placement and strength of individual levels has a strong influence on the average capture rate as a function of temperature. The numerical average from the present data is shown in Fig. 9. It rises to a 5.4-mb peak near $kT = 20$ keV. Uncertainty in the resonance parameters contributes a 10% uncertainty in the average near $kT = 10$ keV and 25% near 30 keV and then rises to ~30% at 100 keV.

Two previous experiments directed at the average capture cross section have been reported. Leugers[39] observed no resonances in capture or transmission and assigned a value of 1 ± 1 mb based on the experimental sensitivity. Beer, Käppeler, and Penzhorn[40] gave a preliminary value of 4.6 ± 0.7 mb for a neutron spectrum approximating $kT = 25$ keV using the activation technique with a clathrate sample. This value compares well with the present result, 5.1 ± 1.2 mb at 25 keV (see Fig. 9). The present 30-keV thermal average value of 4.8 ± 1.2 mb can also be taken as representative of the present experimental and calculational status. Walter, Käppeler, and Bao,[41] for instance, have obtained a preliminary value of 5.6 ± 0.7 mb at $kT = 30$ keV by using a Van de Graaff accelerator, time-of-flight techniques, and two C_6D_6 γ-ray detectors.

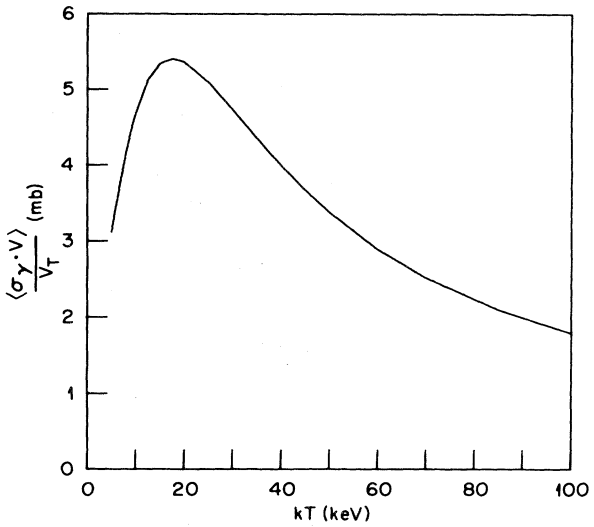

FIG. 9. The effective total neutron capture cross section of ^{86}Kr for neutrons with a Maxwellian energy distribution has been calculated as a function of the energy, kT. See Ref. 36 for further definition of the various quantities plotted here. The uncertainty of the curve amounts to about 10% at $kT = 10$ keV and 25% at $kT = 30$ keV.

The continuing interest in ^{86}Kr and its neighboring nuclides lies in the parameters of stellar nucleosynthesis models. The neutron capture buildup of the heavier elements [the s-process of B^{2}FH (Ref. 42)] branches at ^{85}Kr because of competition with β decay to ^{85}Rb. As the β-decay rate is essentially independent of stellar temperature, the branching ratio is sensitive to the neutron flux or density at the site(s) of the stellar s process. The simple astrophysical picture has been clouded by details such as further branching[43] at ^{86}Rb, ^{89}Sr, and ^{90}Sr in the pulsed neutron production models suggested by Cosner *et al.*[6] Also, the assumption[6] that "the influence of the r-process is rather small in this mass region..." seems to have been negated recently by Cameron.[44] He attributes 41% of the ^{86}Kr abundance to r-process activity either in ordinary stars or in supernovas, while he recognizes the probable importance of intermediate processes in which neutron capture almost always competes with β decay.

The basic problem seems to be that all the above

models predict much more ^{86}Kr than is found in the earth or in meteorites. The latest calculation[43] gives an overproduction factor of 2.4. If Cameron's recent assignment of 41% of the ^{86}Kr abundance to the *r* process is accepted, this factor would increase to $\approx$4.1. One can still hope that further measurements of the other rate constants, temperature, and model dependencies of the ^{85}Kr nucleosynthesis branch will bring a concordant solution. It is clear from the present results (Fig. 9) that a shift of temperature away from the traditional $kT = 30$ keV will not solve the ^{86}Kr overproduction problem.

IV. CONCLUSION

High-resolution neutron resonance spectroscopy has been employed to study especially the 0–250 keV energy window above the neutron binding energy of ^{87}Kr. The neutron resonances in this region have been identified, and many of their properties have been determined. This knowledge has enabled a proper interpretation of the decay scheme, which was constructed by detecting γ rays and neutrons subsequent to the β decay of ^{87}Br. A consistent picture of the physical process has now emerged. On the one hand, delayed neutron spectroscopy in this case is capable of yielding information on individual unbound levels. On the other hand, β decay to the unbound levels is consistent with the assumption of Porter-Thomas distributions for the fluctuation of reduced β transition probabilities about the average β-strength function. The fact that a statistical simulation of a delayed neutron spectrum yields results closely resembling measured data points is not a sufficient reason for disregarding the discrete nature of all strong lines in the measured spectra. The key missing element in previous debates (see Introduction) about the physical meaning of the peak structure in delayed neutron spectra has been the true level density. This quantity cannot be predicted accurately and can be obtained only through detailed measurements such as resonance neutron spectroscopy. It has been shown in this paper that a value approaching the true level density can also be obtained from a detailed decay scheme based on γ ray and delayed neutron data—provided that due caution is exercised. In general, nuclei emitting delayed neutrons cannot be reached through neutron resonance reactions because the corresponding targets are unstable. Besides ^{87}Kr, the only other nucleus that is a daughter of a delayed neutron precursor and that is also accessible with neutrons on a stable target is ^{137}Xe. Measurements with an enriched ^{136}Xe gas target are now in progress at ORELA. Because the neutron-emitting levels in ^{137}Xe have relatively high spins[4] ($5/2^{\pm}$, $7/2^{\pm}$, $9/2^{\pm}$), the overlap between β decay and resonance neutron spectroscopy (which favors low spins) in ^{137}Xe is not *a priori* expected to be as clean or as dramatic as in ^{87}Kr. Therefore ^{87}Br decay is a singular case indeed.

ACKNOWLEDGMENTS

The authors wish to thank R. Winters for providing the computer code MAXWL for calculations of effective capture cross sections and S. G. Prussin for making available the results of theoretical calculations of β strengths. They also thank D. A. McClure and G. G. Slaughter for computer programs that automatically generated Tables III–VI from punched cards. The assistance of C. W. Nestor, Jr., in generating Fig. 8 is gratefully acknowledged. R. W. Sharpe provided editorial assistance. This work was sponsored by the Division of Basic Energy Sciences, U.S. Department of Energy; by the Swedish Natural Science Research Council; and by the German Bundesministerium für Forschung und Technologie. The first-mentioned sponsorship is covered by contract W-7405-eng-26 with the Union Carbide Corporation, which operates the Oak Ridge National Laboratory.

---

*Permanent address: The Studsvik Science Research Laboratory, S-611 82 Nyköping, Sweden.

[1]F. M. Nuh, D. R. Slaughter, S. G. Prussin, H. Ohm, W. Rudolph, and K.-L. Kratz, Nucl. Phys. **A293,** 410 (1977).

[2]O. K. Gjøtterud, P. Hoff, and A. C. Pappas, Nucl. Phys. **A303,** 295 (1978).

[3]J. C. Hardy, B. Johnsson, and P. G. Hansen, Nucl. Phys. **A305,** 15 (1978).

[4]H. Ohm, M. Zendel, S. G. Prussin, W. Rudolph, A. Schröder, K.-L. Kratz, C. Ristori, J. A. Pinston, E. Monnand, F. Schussler, and J. P. Zirnheld, Z. Phys. **A 296,** 23 (1980).

[5]S. G. Prussin, Z. M. Oliveira, and K.-L. Kratz, Nucl. Phys. **A321,** 396 (1979).

[6]K. Cosner, I. Iben, Jr., and J. W. Truran, Astrophys. Lett. **238,** L91 (1980); and private communication.

[7]J. P. Wefel, D. N. Schramm, J. B. Blake, and D.

Pridmore-Brown, Astrophys. J. Suppl. Ser. **45,** 565 (1981)

[8]F. Käppeler and B. Leugers, in *Proceedings of the Specialist's Meeting on Neutron Cross Sections of Fission Product Nuclei,* Bologna, 1979, edited by C. Coceva and G. C. Panini, Comitato Nationale Energia Nucleare Report MEANDC(E) 209 "L", p. 69.

[9]H. T. Maguire, Jr., H. M. Fisher, and R. C. Block, in *Neutron Nuclear Data* (Proceedings of an International Conference, Harwell, 1978), p. 472.

[10]R. L. Macklin and B. J. Allen, Nucl. Instrum. Methods **91,** 565 (1971).

[11]R. L. Macklin, Oak Ridge National Laboratory Report No. ORNL/TM-4810, 1975 (unpublished), and Nucl. Sci. Eng. **59,** 12 (1976) Appendix.

[12]J. Halperin, C. H. Johnson, R. R. Winters, and R. L. Macklin, Phys. Rev. C **21,** 545 (1980).

[13]N. M. Larson and F. G. Perey, Oak Ridge National Laboratory Report No. ORNL/TM-7485, 1980 (unpublished).

[14]G. F. Auchampaugh, Los Alamos Scientific Laboratory Report No. LA-5473-MS, 1974 (unpublished).

[15]C. H. Johnson and R. R. Winters, Phys. Rev. C **21,** 2190 (1980).

[16]G. Rudstam, Nucl. Instrum. Methods **139,** 239 (1976).

[17]K. Aleklett, E. Lund, and G. Rudstam, Z. Phys. A **290,** 173 (1979)

[18]P. Hoff, private communication.

[19]H. Tovedal and B. Fogelberg, Nucl. Phys. **A252,** 253 (1975).

[20]*Table of Isotopes,* 7th Ed., edited by C. M. Lederer and V. S. Shirley (Wiley, New York, 1978); P. Luksch and J. W. Tepel, Nucl. Data Sheets **27,** 389 (1979).

[21]K. Haravu, C. L. Hossas, P. J. Riley, and W. R. Coker, Phys. Rev. C **1,** 938 (1970).

[22]N. A. Detorie, P. L. Jolivette, C. P. Browne, and A. A. Rollefson, Phys. Rev. C **18,** 991 (1978).

[23]C. M. Jensen, R. G. Lanier, G. L. Struble, L. G. Mann and S. G. Prussin, Phys. Rev. C **15,** 1972 (1977).

[24]S. Raman and N. B. Gove, Phys. Rev. C **7,** 1995 (1973).

[25]M. Mizumoto, S. Raman, R. L. Macklin, G. G. Slaughter, J. A. Harvey, and J. H. Hamilton, Phys. Rev. C **19,** 335 (1979).

[26]T. Fuketa and J. A. Harvey, Nucl. Instrum. Methods **33,** 107 (1965).

[27]S. F. Mughabghab, M. Divadeenam, and N. E. Holden, *Neutron Cross Sections,* Vol. 1, Part A (Z = 1–60) (Academic, New York, 1981).

[28]H. Fiedeldey and W. E. Frahn, Ann. Phys. (N.Y.) **19,** 428 (1962).

[29]S. Raman, C. A. Houser, T. A. Walkiewicz, and I. S. Towner, At. Data Nucl. Data Tables **21,** 567 (1978).

[30]D. H. Wilkinson, Nucl. Phys. **A377,** 474 (1982).

[31]S. G. Prussin, private communication.

[32]V. P. Aleshin, Izv. Akad. Nauk SSSR, Ser. Fiz. **37,** 1959 (1973).

[33]H. V. Klapdor and C.-O. Wene, Astrophys. J. **230,** L113 (1979).

[34]J. E. Lynn, *The Theory of Neutron Resonance Reactions* (Clarendon, Oxford, 1968).

[35]C. Gaarde, J. S. Larsen, M. N. Harrakeh, S. Y. Van der Werf, M. Igarashi, and A. Müller-Arnke, Nucl. Phys. **A334,** 248 (1980).

[36]B. J. Allen, R. L. Macklin, and J. H. Gibbons, Adv. Nucl. Phys. **4,** 205 (1971).

[37]J. A. Holmes, S. E. Woosley, W. A. Fowler, and B. A. Zimmerman, At. Data Nucl. Data Tables **18,** 305 (1976).

[38]M. J. Harris, Astrophys. and Space Sci. **77,** 357 (1981).

[39]B. Leugers, Kernforschungszentrum Karlsruhe Report KfK 2895, 1979.

[40]H. Beer, F. Käppeler, and R. D. Penzhorn, quoted by H. Beer and F. Käppeler, in *Neutron-Capture Gamma-Ray Spectroscopy and Related Topics 1981,* edited by T. von Egidy, F. Gönnenwein, and B. Maier (Inst. of Physics, Bristol, 1982), p. 558.

[41]G. Walter, F. Käppeler, and Z. Y. Bao, Kernforschungszentrum Karlsruhe Report KfK 3427, 1982, p. 8.

[42]E. M. Burbidge, G. R. Burbidge, W. A. Fowler, and F. Hoyle, Rev. Mod. Phys. **29,** 547 (1957).

[43]F. Käppeler, H. Beer, K. Wisshak, D. D. Clayton, R. L. Macklin, and R. A. Ward, Astrophys. J. **257,** 821 (1982).

[44]A. G. W. Cameron, Astrophys. and Space Sci. **82,** 123 (1982).